Defence Science Journal, Vol. 70, No. 4, July 2020, pp. 448-453, DOI : 10.14429/dsj.70.15377

Constitutive Equations for Microstructural Features Developed During Solid Particle Erosion of 52100 Steel

Prantik Mukhopadhyay
DRDO-Defence Metallurgical Research Laboratory, Hyderabad - 500 058, India
E-mail: prantikmukherje@yahoo.com

ABSTRACT

Solid particle erosion of the 52100 bearing steel induced the normal growth of the tempered lath martensite, the low angle boundaries and the recovery islets. Microstructural features were revealed using the electron microscopy. Constitutive equations for the normal growth of the tempered lath martensite, energies of the low angle boundaries, and size of the recovery islets have been derived. The normal growth rate of the tempered lath martensite has been derived from the oriented mobility of the boundary in crystallite-stress fields, the driving force from the boundary energy and the pinning force from the uniformly distributed precipitates. Read-Shockley equation has been redefined using the dislocation density term as the misorientation of the boundary. An advanced Read-Shockley equation has been used for predicting the size of the recovery islets (0.12 μm to 0.27 μm) from the local energy equilibrium of the recovered tempered lath martensite, and validated by the TEM bright field microscopic study.

Keywords: Steel; Bearing; Solid particle erosion; Microstructural feature; Constitutive equation; Electron microscopy

1. INTRODUCTION

Cone shaped silica sand particles are used for impacting the target material during the solid particle impact erosion and therefore, the concomitant erosion process is not similar to the liquid impact erosion and slurry erosion. In this process the contact time between particles and the target material is ephemeral, which is known to distinguish the solid particle erosion from the sliding wear, abrasive wear, grinding and machining, where the contact is continuous[1,2].

Engines of the helicopter used in the dusty terrain[3], the rocket motor trail nozzle[4], and equipment of oil and mining industries are often exposed to the solid particle erosion[5,6]. The erosion is severe in the dusty environments due to the ingestion of sand particles in rotating equipment. The thrust vector controlled sophisticated rockets, defence aircrafts and missiles require bearings with greater flexibility[7].

The stress during the erosion is multi-directional and compressive. The confined plastic zone during erosion is known to develop the constrained plastic flow surrounding the indenting particles in the presence of very high compressive stresses, which ensure the larger plastic strains greater than tensile strains. The crucial process parameters of the solid particle erosion are the estimated strain and strain rate, which are of the order of (0.1-1) and (10^3-10^6) s^{-1}.

The high localised stress and ultra-high strain rate of the erosion have been found to induce the normal growth of the tempered lath martensite, the low angle boundaries and the recovery islets in the 52100 bearing steel gradually evolving the thermal energy[1]. The constitutive equations for the normal growth of the tempered lath martensite, energies of the low angle boundaries and the size of the recovery islets developed in the 52100 bearing steel have been derived in this work and validated by electron microscopy, in order to design and develop flexible and tougher bearings.

2. MATERIAL AND METHODS

The composition of the alloy used for experiments is the 52100 bearing steel shown in the Table 1. The inductively coupled plasma optical emission spectrometer and the LECO instruments were used for analysing the composition.

Table 1. Composition (in Weight Percent) of 52100 steel

C	Mn	Si	Cr	Mo	Ni	S	P	Fe
1.00	0.30	0.36	1.46	0.004	0.03	0.01	0.01	Balance

The home grown knowledge based hardening and tempering treatments were employed to develop the tribological properties. The hardening treatment was performed by solutionising at 850 °C, soaked for 1h/in and followed by oil quenching. The tempering was done at 300 °C, soaked for 2h/in, and followed by the air cooling. The solid particle impact erosion RIG experiment was performed according to the ASTM standard ASTM G 76-83. Silica sands of size 200±50 μm were used for impacting the target 5x4x1 cm^3 52100 bearing steel specimen at 105 m s^{-1} machine estimated velocity and at an angle 45°. The steady state erosion rate became tangible after the erosion for 45 min corresponding to 70 g of the erodent.

Received : 07 February 2020, Revised : 20 April 2020
Accepted : 28 May 2020, Online published : 13 July 2020

The Electron Backscatter Diffraction (EBSD) study was done by the Carl Zeiss make SUPRA 55, Scanning Electron Microscope with the Field Emission Gun to measure the character of predominant phases qualitatively. The electro-polished TEM samples were used for the EBSD study with the step size 0.10-0.12 μm . Special BCT phase parameter file, shown in Table 2, was used for detecting the martensite precisely. This has been done after being confirmed, by rigorous trial experiments, that the use of the BCC phase parameter file generated higher mean angular deviations of the Kikuchi patterns, than the BCT phase parameter file, for the known martensitic structure. The character of predominant phases were measured and represented.

Table 2. The BCT phase crystal structure parameter file

L_1 (nm)	L_2 (nm)	L_3 (nm)	Atom positions	Space group
0.285	0.285	0.298	(000), $\left(\frac{1}{2}\frac{1}{2}\frac{1}{2}\right)$	I4 mmm (I-139)

The normal TEM sampling technique was used for preparing 3 mm diameter and 100 μm thick samples by precise grinding to the surface just beneath the worn out surface. The Twin Jet electro-polisher was used for electro-polishing using 75% Methanol, 10% H_2SO_4, 10% Lactic Acid, 3% HNO_3 and 2% HF solution. The precise grinding and electro-polishing of samples ruled out the chance to encounter worn out debris during the TEM study. The TEM study was performed using the Bright Field Microscopy of FEI TECHNAI G^2 microscope.

3. CONSTITUTIVE EQUATIONS

3.1 Normal Growth of the Tempered Lath Martensite

Large number of smaller size martensite laths was found in as received state (Fig. 1(a)). The discontinuous normal growth of the tempered lath martensite during the erosion was revealed in EBSD study (Fig 1(b)), which was confirmed by the TEM bright field study, represented by (Fig. 2 (a)).

The boundary energy per unit volume of tempered lath martensite is written as

$$F_K = \frac{\lambda\gamma}{R} \tag{1}$$

where γ is the surface energy per unit area, R is the radius of lath boundary and λ is a geometric constant[8].

Growth velocity (v) of boundaries[9,10] is generally defined by lath boundary energy driving force (F_K) and boundary mobility (J) where

$$v = \frac{dR}{dt} = JF_K = \frac{J\lambda\gamma}{R} \tag{2}$$

Mobility of the boundary is represented as[11]

$$J = \eta\, J_0 \exp\left(-\frac{H(\theta)}{kT}\right) \tag{3}$$

where J_0 is the intrinsic mobility, η is the pre-exponential orientation based factor, k is the Boltzmann constant, T is the temperature and $H(\theta)$ is the oriented activation energy based on the boundary angle.

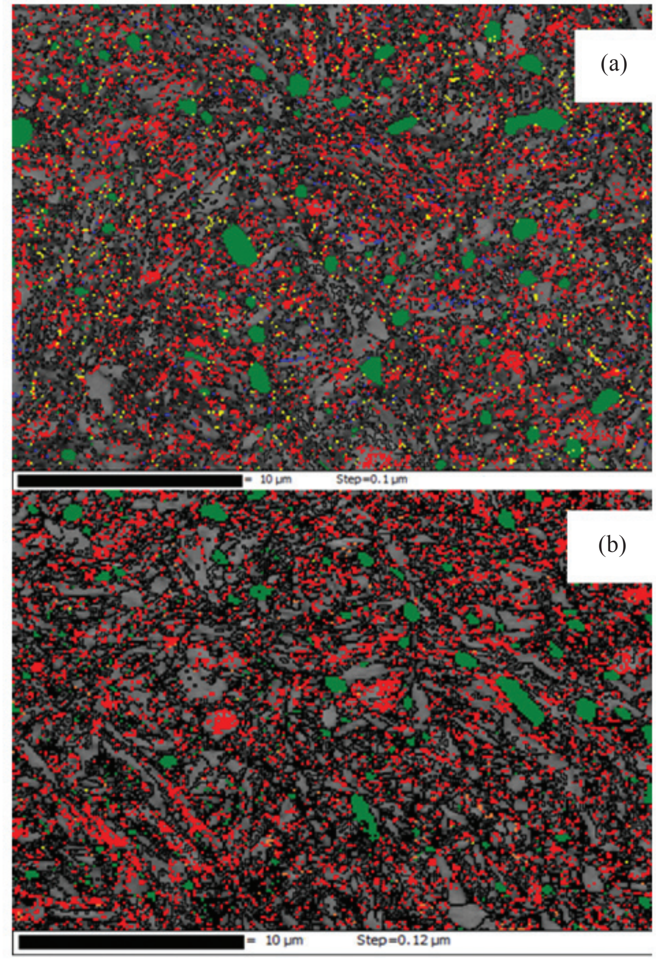

Figure 1. EBSD measured phase character (a) As received sample, (b) Solid particle 45° impact deformed sample. Martensite lath: Band Contrast, Fe_3C: Green, $Cr_{23}C_6$ and Cr_7C_3: Red, Mn_5C_2: Yellow.

Back driving force exerted by fine precipitates on the boundary[9,10,11] during growth is

$$j_h = \frac{3f_v\gamma}{2r} \tag{4}$$

where f_v is the volume fraction of the fine precipitates and r is the radius of precipitates.

Resulted the driving force per unit volume is

$$F_{KT} = \left(\frac{\lambda\gamma}{R} - \frac{3f_v\gamma}{2r}\right) \tag{5}$$

Therefore the effective normal growth velocity of martensite boundary pinned by the uniformly distributed precipitates is

$$v = \frac{dR}{dt} = JF_{KT} = \eta\, J_0 \exp\left(-\frac{H(\theta)}{kT}\right)\left(\frac{\lambda\gamma}{R} - \frac{3f_v\gamma}{2r}\right) \tag{6}$$

Magnitude of crystallite shear-stress field (τ) due to applied external normal stress (σ) is generally expressed using orientation based Taylor factor (T_t)

$$\tau = \frac{\sigma}{T_t} \tag{7}$$

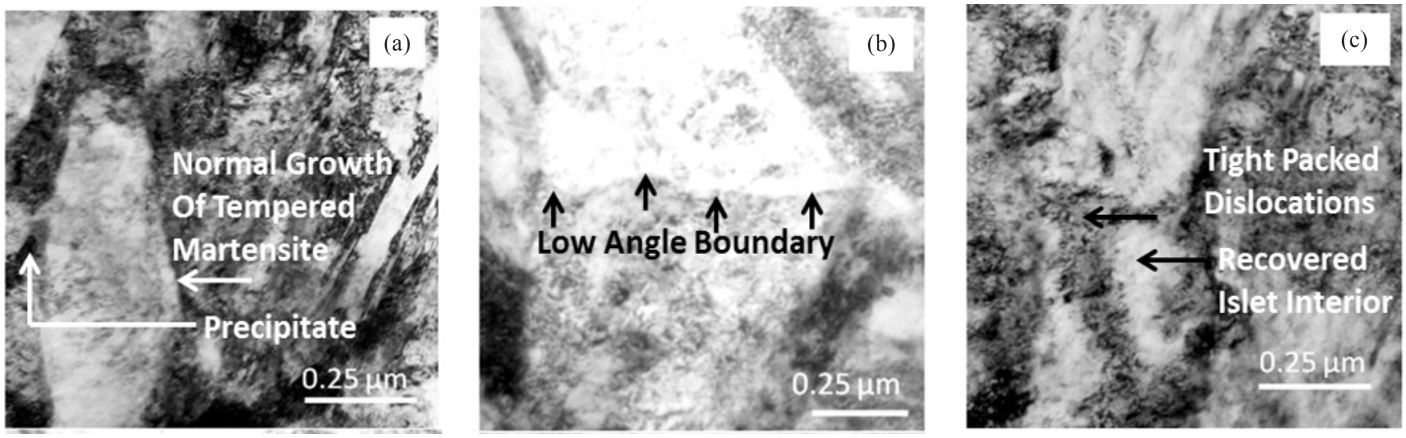

Figure 2. Solid particle impact erosion induced microstructural features (a) Normal growth of tempered lath martensite pinned by precipitates, (b) Development of low angle boundary, (c) Recovery islets of tempered martensite.

Crystallite-stress field helps the atoms for crossing the activation energy hill, defined by the crystallite-stress induced high elastic free energy and to settle in the new stable locations. Therefore, the resultant velocity of boundary is derived as the original enthalpy induced activation energy hill, corrected by additional elastic energy from applied stress

$$v = \frac{dR}{dt} = \eta\ J_0\ \exp\left(-\frac{\left(H(\theta) - \frac{K_R \sigma}{T_t} \right)}{kT} \right) \left(\frac{\lambda\gamma}{R} - \frac{3 f_v \gamma}{2r} \right) \quad (8)$$

where the K_R is the activation volume. Magnitudes of the range for short range stresses are known to be less than 5-10 interatomic distances[12]. Therefore, the crystallite volume is under short range stresses, resulted from scattered dislocations or loosely tangled dislocations of low angle boundaries, when K_R is ranging from less than $(5b)^3$ to $(10b)^3$.

3.2 Energy of the Low Angle Boundaries

The development of the low angle boundaries during erosion was revealed in the TEM study, represented by Fig. 2(b). The misorientation angle θ (in radian) of a symmetrical tilt boundary constituted by edge dislocations with the dislocation spacing *d* is written as[13]

$$\tan\theta = \frac{b}{d} \quad (9)$$

where *b* is the burger vector.

The dislocation density is generally defined by the total length of dislocations per unit volume with the unit L^{-2} where *L* is the length scale. Therefore, the dislocation spacing of a symmetrical tilt boundary with the dislocation density ρ_b is denoted by

$$d^{-2} = \rho_b \text{ and hence}$$

$$d = \frac{1}{\rho_b^{\frac{1}{2}}} \quad (10)$$

Hence, the misorientation angle of a symmetrical tilt boundary is written as

$$\theta = \tan^{-1}\left(\frac{b}{d}\right) = \tan^{-1}\left(b\rho_b^{\frac{1}{2}}\right) \approx b\rho_b^{\frac{1}{2}} \quad (11)$$

The Read-Shockley equation for a tilt boundary[13] is

$$E = \frac{\theta\ G\ b}{4\pi(1-\upsilon)}\left[1 + \ln\left(\frac{b}{2\pi\ r_0}\right) - \ln\theta\right] \quad (12)$$

where r_0 is the dislocation core radius ranging from *b* to 5b, υ is the ratio of transverse strain to longitudinal strain and G is the shear constant. It is the force per unit length or energy per unit area of the low angle grain boundary.

Therefore, resulting boundary energy per unit area of a tilt boundary with the dislocation density, ρ_b is written as

$$E_D = \frac{Gb^2\rho_b^{\frac{1}{2}}}{4\pi(1-\upsilon)}\left[1 + \ln\left(\frac{b}{2\pi\ r_0}\right) - \ln\left(b\rho_b^{\frac{1}{2}}\right)\right] \quad (13)$$

The misorientation angle of a twist boundary constituted by the screw dislocations has been postulated in literature as

$$\theta \approx \frac{b}{d} \quad (14)$$

when two screw dislocations merged to be one[13]. Thus, the advanced Read-Shockley equation for a twist boundary is

$$E_{DT} = \frac{Gb^2\rho_b^{\frac{1}{2}}}{4\pi}\left[1 + \ln\left(\frac{b}{2\pi\ r_0}\right) - \ln\left(b\rho_b^{\frac{1}{2}}\right)\right] \quad (15)$$

3.3 Size of the Recovery Islets

The occurrence of the recovery islets of the tempered martensite during erosion has been revealed in TEM bright field study, represented by Fig. 2(c). For the recovered microstructure the volume free energy (ΔG_V) defined by the mean dislocation density (ρ_r) of the bulk should be sufficient to balance the energy (*E*) of the low angle boundaries of recovery islets. For recovery islets size R_D

$$\frac{4}{3}\pi\ R_D^3 \Delta G_V = 4\pi\ R_D^2 E \quad (16)$$

Therefore, the size of the recovery islets is

$$R_D = \frac{3E}{\Delta G_V} = \frac{3Gb^2\rho_b^{\frac{1}{2}}}{2\pi Gb^2\rho_r}\left[1+\ln\left(\frac{b}{2\pi\ r_0}\right)-\ln\left(b\ \rho_b^{\frac{1}{2}}\right)\right] = \frac{3\rho_b^{\frac{1}{2}}}{2\pi\rho_r}\left[1+\ln\left(\frac{b}{2\pi\ r_0}\right)-\ln\left(b\ \rho_b^{\frac{1}{2}}\right)\right] \tag{17}$$

where the ρ_b is the dislocation density of the low angle boundary and ρ_r is the mean dislocation density of the bulk recovered microstructure.

4. DISCUSSION

4.1 Normal Growth of the Tempered Lath Martensite

The as received state was with high surface energy from the high angle boundaries, which would have been the driving force for the extensive discontinuous growth. The growth of the tempered lath was brought to the normalcy by the pinning force from the uniformly distributed precipitates and less boundary energy per unit volume of the straight lath boundaries with larger radius of lath martensite, R (Fig. 1(b) and Fig. 2(a)).

The driving force of Burke and Turnbull equation is redefined using pinning force from precipitates. The oriented kinetics of grain boundaries is known to be changed by the boundary misorientation, which is liable to control the pre-exponential intrinsic mobility and the exponential enthalpy[10].

The boundary kinetics due to the presence of stress suggested that the mobility of boundary was enhanced if the shear stress direction tallied with advancing boundary and lateral growth of boundary should not be possible by the stress applied normally[14]. In contrary, the micro-mechanism based crystal plasticity suggests that for every applied external stress the individual crystallites develop their own crystallite-stress fields, where the directionality of the crystallite-stress fields is governed by the crystallite orientation, in regard to the applied stresses. The crystallite-stress fields increase the internal energy and therefore, the elastic strain energy, which will liable to control the mobility of lath boundary. For the low angle boundaries the mobility is predominantly defined by the diffusion of atoms, while for the high angle boundaries though the diffusion is a recognised phenomenon but their kinetics is not as simple as the diffusion. However, both the diffusivity and mobility should have been governed by the crystallite-stress fields. For instance the crystallite-stress fields induce atomic vibration in bonding. Therefore, the requirement of the thermal activation energy in form of the enthalpy is liable to decrease in the exponential term of the mobility. The crystallite-stress fields definitely carry the freedom to certain orientations of high crystallite-stress to compensate the less mobility of the adjacent slow moving boundaries during metal working. For a certain applied normal stress, the orientations with high T_t will have comparatively less localised shear-stress field to promote the grain boundary mobility during high strain and strain rate tribological processes. From the principle of work hardening the high T_t is known to provide a greater magnitude of slip and a higher internal energy by the localised crystallite-strain, which is liable to change the range of the crystallite-stress fields K_R. Other than that, the high strain and strain rate of the tribological process induce the thermal energy, which is generally resulted in the dynamic recovery of dislocations. In the hot working the plastic strain field is minimised reducing the localised strain and developing of the stable energy state defined by the low angle grain boundaries. The development of the low angle boundaries and the annihilation of dislocations are less during the erosion, when the evolved thermal energy is less but the dislocation recovery occurs[1]. The crystallographic orientation dependent recovery is equally crucial for the existence of versatile crystallite-stress fields K_R, which ought to control the kinetics of lath boundaries.

4.2 Energy of the Low Angle Boundaries

The plastic deformation is known to increase the dislocation density[9,10,15]. The increase of dislocation density is liable to reduce the spacing between individual dislocations. Generally the dislocation density is well known as the total length of dislocations per unit volume with the unit L^{-2}. Therefore, the mean spacing of dislocations is expressed as $d^{-2} = \rho_b$.

The elastic strain energy of dislocations is liable to increase the volume free energy and to reduce the stability. The low angle grain boundaries are formed to stabilize the energy state (Fig. 2(b)). This stable state may be developed by pure edge dislocations or screw dislocations. Consequently they develop the tilt and twist boundaries[9,13]. The misorientation of these low angle grain boundaries is generally defined by the equation $\theta \approx \frac{b}{d}$. This equation is well known for the symmetrical tilt boundaries but could be used for the twist boundaries, where two types of pure screw dislocations, merge to be one screw dislocation. As said earlier, the mean dislocation spacing is known to be changed by the mean dislocation density of the boundary. Hence, the misorientation of the low angle grain boundary is redefined by the dislocation density of the boundary, where $\theta = b\rho_b^{\frac{1}{2}}$.

4.3 Size of the Recovery Islets

The plastic deformation during the erosion has been observed to develop the recovery islets (Fig. 2 (c)). The crystallographic orientation dependent recovery islets are developed during the deformation by the dynamic recovery. The local energy equilibrium tells that the volume free energy from the mean dislocation density of the bulk, should be sufficient to balance the surface energy of the developed recovery islets, confined by the tightly packed dislocations boundary (Fig. 2(b)). The mean dislocation density (ρ_r) of the islet interior is less than the dislocation density of the islet boundary (ρ_b). The surface energy of the recovery islet boundaries is represented by the advanced version of Read-Shockley equation, using the dislocation density term as the misorientation of the islet boundaries.

5. VALIDITY OF THE CONSTITUTIVE EQUATIONS FROM THE ELECTRON MICROSCOPIC EXPERIMENTS

The normal growth of the tempered lath martensite is revealed in Fig. 1(b) and Fig. 2(a). The growth was discontinuous. The pinning of lath boundary by the uniformly distributed precipitates brought the growth normalcy, revealed by EBSD measured phase character, Fig. 1(b). The discontinuous bulging of the lath boundary from the precipitate free place revealed the existence of the particle pinning, Fig. 2(a). The solid particle impact erosion was performed at an angle 45° by the irregular shaped sand particles, which developed the multidirectional stress and the constrained plastic flow. The bulging of the lath boundary did not resemble any uniform macro-flattening trend in the microscopic multidirectional stress environment. Therefore, the normal growth of lath boundaries is controlled by the oriented mobility of the boundary in crystallite-stress fields, driving force from the boundary energy and the pinning force from the uniformly distributed precipitates.

The solid particle impact erosion at a steady state with the angular impact enabled to produce the low angle boundary, Fig. 2(b), which resembled polygonised boundary with the both tilt and twist boundaries. Read-Shockley equation to derive the strain energy of low angle boundaries per unit area was estimated from the strain energy of the individual dislocation per unit length, multiplying with the total number of dislocations per unit area. The dislocation density is known to be the total length of dislocations per unit volume. Therefore,

the dislocation density is represented as the number of dislocations per unit area. The misorientation angle of the low angle boundaries increases with the increase of the dislocation density. Hence, the length scale of dislocation spacing has been redefined as the dislocation density to replace misorientation angle. Therefore, the advanced Read-shockley equations are liable to be used for the low angle boundaries.

The size of recovery islets of the tempered martensite has been derived from the equilibrium of the volume free energy and the surface free energy, which has been estimated using the advanced Read-Shockley equation. The shear constant, G, of the hardened and tempered 52100 bearing steel has been considered to be 80 GPa and the b vector has been considered to be 0.25 nm. The size of the recovery islets of the tempered lath martensite has been derived to be 0.12 to 0.27 μm, when the mean dislocation density of the bulk after recovery is of the order of 10^{15} m^{-2} and the dislocation density of the islet boundary is 10^{16} m^{-2}. The TEM bright field microscopy was used for validating the size of the recovery islet. Fig. 2(c) is legitimately validating the size of recovery islet, 0.2 μm, of the tempered lath martensite.

The solid rocket motors are generally used for space rockets and missiles. The flexibility of composite bearings reinforced with tougher steels is usually known to be very crucial for thrust vector controlled solid rocket motors[7]. The plastic flow properties of the tribological steels are usually represented by their toughness. The erosion resistance of the ferritic steel with greater toughness, were found to be superior than the martensitic steel, with less toughness[1,15]. The composition of the steel is liable to decide the microstructure for the same processing history, while the composition and microstructure are known to control the toughness. The plastic work done during erosion on the surface of the tribological steels is liable to induce the normal growth of lath martensite, the low angle boundaries and the recovery islets, which control the plastic flow behavior and induce toughness[1,15]. Therefore, the genesis of the microstructural development is required to be quantified to enhance the erosion resistance property by suitable alloy design.

6. CONCLUSIONS

(i) Normal growth of the tempered lath martensite during the erosion has been redefined by the oriented mobility of boundary in the crystalite-stress fields, the driving force from boundary energy and the pinning force from the uniformly distributed precipitates.

(ii) Dislocation spacings of the low angle boundaries have been expressed as the dislocation density of the boundary.

(iii) Energies of the low angle boundaries have been defined using the dislocation density term, replacing the misorientation angle.

(iv) Size of the recovery islets, 0.12-0.27 μm, of the tempered martensite has been predicted from the local energy equilibrium between the volume free energy and the surface energy, derived from advanced Read-Shockley equation.

(v) Constitutive equations have been validated by electron microscopy.

Conflicts of Interest

Author would like to declare that he don't have any personal, financial and other conflicts of interest, which have the importance for compromise or bias objectivity or professional judgment.

REFERENCES

1. Mukhopadhyay, P.; Srinivas, M. & Roy, M. Microstructural developments during erosion of tribological steels. *Mat. Char.,* 2016, **113**, 43-51.
   doi: 10.1016/j.matchar.2016.01.008
2. Chen, Q. & Li, D. Y. Computer simulation of solid particle erosion. *Wear*, 2003, 254 (3-4), 203-210.
   doi: 10.1016/S0043-1648(03)00006-1
3. Feuerstein, A. & Kleyman, A. Ti-N multilayer systems for compressor airfoil sand erosion protection. *Surf. Coat. Technol.,* 2009, **204**(6-7), 1092-1096.
   doi: 10.1016/j.surfcoat.2009.09.053
4. De Morton, M.E. Erosion in rocket motor nozzles. *Wear,* 1977, **41**(2), 223-231.
   doi: 10.1016/0043-1648(77)90003-5
5. McI Clark, H. & Llewellyn, R.J. Assessment of erosion resistance of steels used for slurry handling and transport in mineral processing applications. *Wear,* 2001, **250**(1-12) 32-44.
   doi: 10.1016/S0043-1648(01)00628-7
6. Gnanavelu, A.; Kapur, N.; Neville, A. & Flores, J.F. An integrated methodology for predicting material wear rates

due to erosion, *Wear,* 2009, **267**(11), 1935-1944.
doi: 10.1016/j.wear.2009.05.001

7. Ram Mohan, CH.V.; Ramanathan, J.; Kumar, S. & Gupta, A.V.S.S.K.S. Characterisation of materials used in flex bearings of large solid rocket motors. *Def. Sci. J.*, 2011, **61**(3), 264-269.
doi: 10.14429/dsj.61.52
8. Burke, J.E. & Turnbull, D. Recrystallization and grain growth. *Prog. Metal Phys.,* 1952, **3**, 220-292.
doi: 10.1016/0502-8205(52)90009-9
9. Huang, Y. & Humphreys, F.J. Measurements of grain boundary mobility during recrystallization of a single-phase aluminium alloy. *Acta. Mater.* 1999, **47**(7), 2259-2268.
doi: 10.1016/S1359-6454(99)00062-2
10. Mukhopadhyay, P.; Leock M. & Gottstein G. A cellular operator model for simulation of static recrsytallization. Acta Mater., 2007, 55(2), 551-564.
doi: 10.1016/j.actamat.2006.08.045
11. Raabe, D. & Hantcherli, L. 2D cellular automaton simulation of the recrystallization texture of an IF sheet steel under consideration of Zener pinning. 2005, **34**(4), 299-313.
doi: 10.1016/j.commatsci.2004.12.067
12. Dieter G. Mechanical metallurgy. SI Metric, McGraw-Hill, London, 1988, p. 141.
13. Hull, D. & Bacon, D.J. Introduction to dislocations. 5th Ed., Elsevier, London, 2011, 163p.
doi: 10.1016/B978-0-08-096672-4.00002-5
14. Winning, M. Grain growth under influence of mechanical stresses. *Z. Metallkd*. 2005, **96**(5), 465-467.
doi: 10.3139/146.018137
15. Mukhopadhyay, P.; Kannaki, P.S.; Srinivas, M. & Roy, M. Microstructural developments during abrasion of M50 bearing steel. *Wear,* 2014, **315**(1-2), 31-37.
doi: 10.1016/j.wear.2014.03.010

ACKNOWLEDGEMENTS

Dr M. Roy, project director of DRDO Project Speciality Steels for Defence Application, DMR-292B, for supplying 52100 bearing steels and for doing erosion experiment is gratefully acknowledged. Director of Defence Metallurgical Research Laboratory, DRDO is gratefully acknowledged for encouragement.

CONTRIBUTOR

Dr Prantik Mukhopadhyay did his PhD from RWTH Aachen University of Germany in the year 2005. He joined DIAT, DRDO on 2nd August 2007 after his postdoctoral work from University of Birmingham, UK and IISc Bangalore. After completing DIAT Grants in Aid project work on Cartridge Brass. Presently he is working as a Scientist 'F' at DRDO-Defence Metallurgical Research Laboratory, Hyderabad, India. He was engaged in many crucial DRDO projects, like Development of High Hardness Bainitic Steel for Hull of the Main Battle Tanks and the Certification of Bulb Bars for Indian Navy. Presently he is engaged in research and analysis of the developed Tribological Steels under the project work Speciality Steels for Defence Application other than the research and analysis work on Quantitative Analysis of Dynamic Recovery of Dislocations for the Development of Nano Bainitic Steel by Ausforming.